

Vascular Medicine

<http://vmj.sagepub.com/>

Endovascular model of abdominal aortic aneurysm induction in swine

Alex Lederman, Fernando Tavares Saliture Neto, Rimarcs Ferreira, Luis Francisco Poli de Figueiredo, Jose Pinhata Otoch, Ricardo Aun and Erasmo Simão da Silva

Vasc Med 2014 19: 167

DOI: 10.1177/1358863X14534006

The online version of this article can be found at:

<http://vmj.sagepub.com/content/19/3/167>

Published by:



<http://www.sagepublications.com>

On behalf of:



Additional services and information for *Vascular Medicine* can be found at:

Email Alerts: <http://vmj.sagepub.com/cgi/alerts>

Subscriptions: <http://vmj.sagepub.com/subscriptions>

Reprints: <http://www.sagepub.com/journalsReprints.nav>

Permissions: <http://www.sagepub.com/journalsPermissions.nav>

>> [Version of Record](#) - May 30, 2014

[What is This?](#)

Endovascular model of abdominal aortic aneurysm induction in swine

Vascular Medicine
2014, Vol. 19(3) 167–174
© The Author(s) 2014
Reprints and permissions:
sagepub.co.uk/journalsPermissions.nav
DOI: 10.1177/1358863X14534006
vmj.sagepub.com



Alex Lederman^{1,2}, Fernando Tavares Saliture Neto², Rimarcs Ferreira³, Luis Francisco Poli de Figueiredo^{4,a}, Jose Pinhata Otoch⁴, Ricardo Aun^{2,5} and Erasmo Simão da Silva⁵

Abstract

Abdominal aortic aneurysms are among the main causes of death. The high morbidity and mortality associated with aneurysm rupture and repair represents a challenge for surgeons and high risk for patients. Although experimental models are useful to understand, train, and develop new treatment and diagnostic methods for this pathology, animal models developed to date are far from ideal. Animals are either too small and do not represent the pathology of humans, or the procedures employ laparotomy, or the aortic behavior does not resemble that of a true aneurysm. We developed a novel, less invasive and effective method to induce true aortic aneurysms in Large White pigs. Animals were submitted to an endovascular chemical induction using either calcium chloride (25%) or swine pancreatic elastase. Controls were exposed to saline solution. All animals were operated on using the same surgical technique under general anesthesia. They were followed weekly with ultrasound examinations and at 4 weeks the aorta was harvested. Although elastase induced only arterial dilation, imaging, histological, and biomechanical studies of the aorta revealed the formation of true aneurysms in animals exposed to calcium chloride. Aneurysms in the latter group had biomechanical failure properties similar to those of human aneurysms. These findings indicate that the endovascular approach is viable and does not cause retroperitoneal fibrosis.

Keywords

aortic aneurysm, biomechanics, calcium chloride, elastase, pig model

Introduction

Abdominal aortic aneurysms (AAAs) are a major health concern today. There has been an increase in incidence with the aging population and a rise in diagnosis due to an increase in the effectiveness, availability, and frequency of imaging procedures (e.g. ultrasound and computed tomography (CT) examinations in the general population). The high morbidity and mortality associated with aneurysm rupture and repair makes it a great challenge for today's surgeons. Live models are necessary to better understand the natural history of aneurysm, test new diagnostic and repair technologies, and provide improved training settings for future surgeons.^{1,2} However, an ideal animal model of aneurysm has not been achieved to date. Most models have been developed in small animals (rodents, rabbits),³ which do not resemble the human model regarding size and hemodynamic, thrombogenic, and immunological differences.^{4,5} In turn, medium to large animal models have been achieved via a surgical procedure with aortic exposure and handling,^{2,5} leading to the formation of scarred retroperitoneal fibrosis, which prevents an ideal training and testing environment for aneurysmal disease. Moreover, in many cases, the arterial dilation models created are not representative of

true aneurysm, as they do not contain all the arterial wall layers characteristic of this condition.^{1,2,4,6,7} Hence, the physiological and pathological behavior of these systems may not resemble those of a natural aneurysm.

¹Vascular Surgery, Hospital Universitário, Universidade de São Paulo (USP), São Paulo, Brazil

²Vascular Surgery, Hospital Israelita Albert Einstein, São Paulo, Brazil

³Pathology, Escola Paulista de Medicina, Universidade Federal de São Paulo, São Paulo, Brazil

⁴Surgical Techniques, Faculdade de Medicina da Universidade de São Paulo (USP), São Paulo, Brazil

⁵Vascular Surgery, Faculdade de Medicina da Universidade de São Paulo (USP), São Paulo, Brazil

^aIn memoriam.

Corresponding author:

Alex Lederman
Hospital Universitário
R Capote Valente, 439 cj 125
São Paulo, SP – 05409-001
Brazil
Email: alexlederman@yahoo.com.br

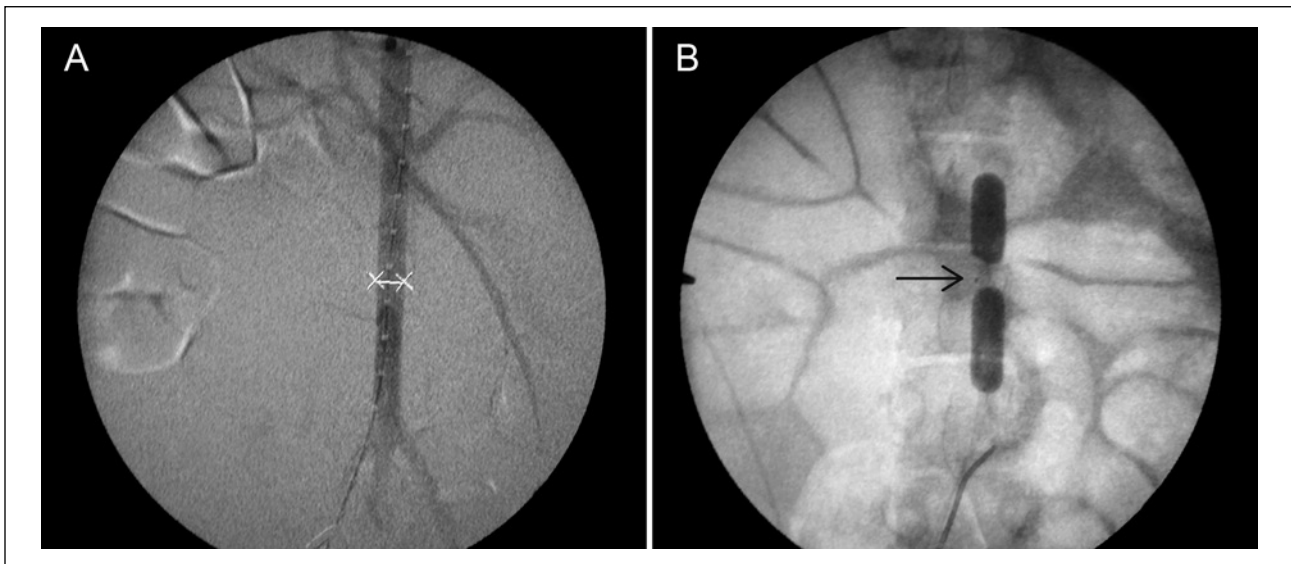


Figure 1. (A) Pig aortography with measurements (X-X 7mm) Pigtail marks 10mm and renal and lumbar arteries. (B) Two Fogarty catheters with insufflated balloons and a microcatheter placed in between (arrow).

Our goal was to describe an endovascular approach to chemically induce true aortic aneurysms in medium–large animals. With this method we were able to successfully induce aortic aneurysms, with biomechanical properties that resemble those of human aneurysms, without retroperitoneal fibrosis.

Materials and methods

This protocol was approved by the Institutional Ethics Committee from the Instituto de Ensino e Pesquisa – Hospital Israelita Albert Einstein and from the Faculdade de Medicina da Universidade de São Paulo. This research was conducted in compliance with the *Guide for the Care and Use of Laboratory Animals* at an AAALAC-accredited facility.

Eighteen Large White pigs weighing an average of 36.5 kg (range: 28–47 kg) were used in this study. The first nine animals were used for ‘fine tuning’ the protocol. Of the remaining nine animals, one was excluded due to sudden death on the first operative day. The remaining eight animals were subdivided into: two control animals, three calcium chloride-treated, and three elastase-treated animals. Doses of treating drugs used were: 0.2 mL of calcium chloride (CaCl_2) 25% (Centro Paulista de Desenvolvimento Farmacotécnico Ltda, São Paulo, SP, Brazil; 10 ml) and 40.8 units (0.2 mL) of swine pancreatic elastase (E-1250-25 mg – 6.25 ml; Lot: 078K7018; Sigma-Aldrich, St Louis, MO, USA).

While still in the stall, all animals were treated with a deep intramuscular dose of midazolam 0.2 mg/kg associated with acepromazine 1% 1 mg/kg as a pre-anesthetic treatment. When the animals were asleep, they were washed (bathed with water and regular soap to remove the dirt) and weighed. Under this sedation, a superficial venous line was punctured in the ear. Through this venous access, all medication was administered. General anesthesia was obtained with propofol infusion (initially 2 mg/kg). After orotracheal

intubation with tube 6.5, inhalation anesthesia was maintained with isoflurane 0.5–1%, with mechanical ventilation (volume flow 10 ml/kg/h; rate of 16 breaths/min).

Once under general anesthesia and after the usual surgical preparation, the femoral artery was exposed. Systemic anticoagulation was performed with 10,000 IU of heparin. Aortography (BV Pulsera, Phillips, The Netherlands) with a 5F centimetered pigtail catheter (Cook Medical, Bloomington, IN, USA) was obtained. Initial aortic diameter and length measurements were taken and renal and lumbar artery positions were identified (Figure 1A). Under the road-mapping technique, two Fogarty 4 catheters (Edward Life Science, Irvine, CA, USA) were positioned over two consecutive pairs of lumbar arteries. A 3F MicroFerret microcatheter (Cook Medical, Bloomington, IN, USA) was placed in between the balloons (Figure 1B). This catheter has a 0.4 mL priming volume, which was filled with the desired agent before the expected dosage was applied. After balloon inflation, half of the treating dose (0.1 mL) was deployed. The second half (0.1 mL) was delivered 7 minutes after the initial dose. After 15 minutes, we retrieved 3 mL of blood and deflated the balloons. A control aortography was done. Femoral artery closure was done with prolene 6-0 suture. Inguinal closure was done with two layers of 3-0 nylon suture. The pigs received silver ointment sprayed over the suture line and 1 g of intravenous cephalotin. They were maintained with water and food ad libitum, and a daily dose of 100 mg of aspirin.

Ultrasound Doppler (Phillips) examinations were performed under general anesthesia on day 0, before surgery, and day 28, before harvesting the aorta. On days 7, 14, and 21 the animals received an intramuscular dose of midazolam (0.2 mg/kg) prior to examination.

Harvested aortas were maintained in saline solution and under a controlled temperature (refrigerator) up to 24 hours before macroscopic measurements were taken and biomechanical tests conducted.

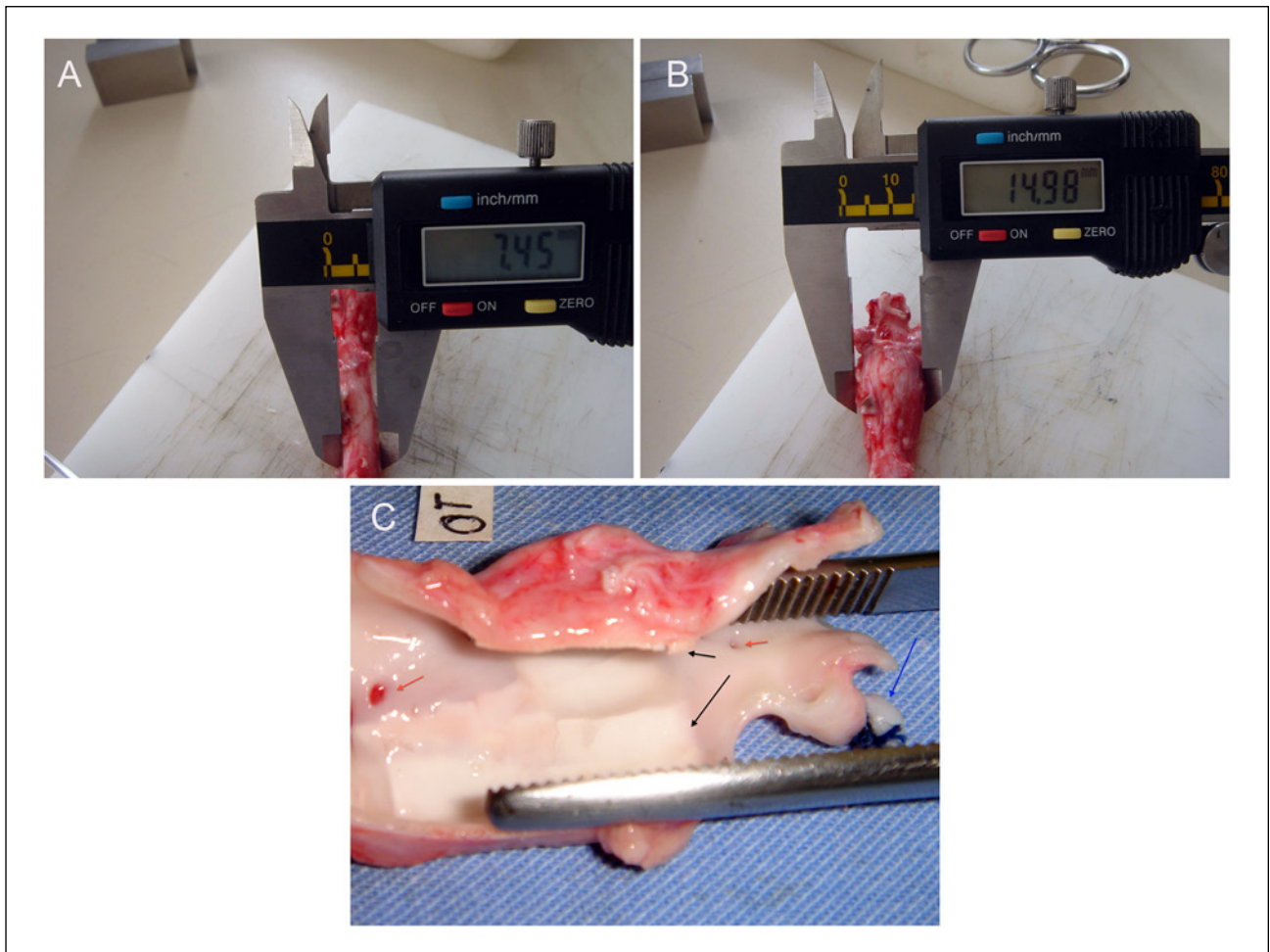


Figure 2. (A) Non-treated segment; (B) calcium chloride-treated segment (same sample as (A)); (C) calcium chloride-treated segment, opened longitudinally: blue arrow indicates left renal artery ligation; black arrows indicate calcified plaques; red arrows show lumbar arteries that define treated area.

Similar parallel fragments were separated for histological and biomechanical tests.

Unidirectional biomechanical destructive tests were done using an Instron Spec 2200, as previously described.^{8,9} An automatic data report was obtained using a Series IX program. Load, displacement, strength, tension, stress, and strain data were reported until the sample ruptured.

Histological studies used hematoxylin-eosin, Verhoeff and Masson stains.

Results

Methodological adjustments

Because side effects (paraplegia, neurogenic bladder, rectal prolapse, and livedo) were observed in the first nine animals, technical adjustments were implemented. The initial dose of CaCl_2 50% was replaced with 0.2 ml of CaCl_2 25% to minimize the likelihood of side effects. Conversely, the initial dose of elastase (27.2 U) was increased to 40.8 U as the original dose did not prove effective to induce aneurysmal dilation. Additionally, dose deployment was also adjusted to prevent washout (half dose per half period – at

0 and 7 minutes after balloon inflation). Similarly, a pigtail catheter (5F) was substituted for a microcatheter (3F), and balloon inflation occurred between two pairs of lumbar arteries (Figures 1B, 2C).

Doppler imaging

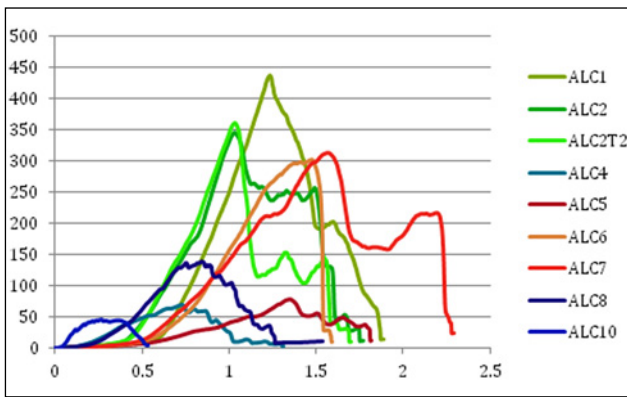
Follow-up Doppler ultrasound images showed progressive dilation over the course of the study. Dilation was highest in animals treated with calcium chloride. Wall calcification was also observed in this group. Dilation was also detectable in animals treated with elastase, although to a lesser extent. Treatment with saline had no effect on the arterial wall (Table 1).

Macroscopic findings

Macroscopic findings showed no retroperitoneal fibrosis in all cases. The CaCl_2 group developed aneurysmal dilation and calcification of the aortic wall (Figure 2A–C), whereas elastase-treated animals showed only a dilated segment. No anatomical changes were observed in control animals.

Table 1. Ultrasound (US) weekly measurements and diameter variation.

Group	Animal		US0	US1	US2	US3	US4
Control	ALC2	Measurement	0.90	1.00	1.03	1.03	0.90
		Variation to initial measurement (%)	–	11.1	14.4	14.4	0.0
	ALC1	Measurement	0.86	0.80	0.80	1.04	0.80
		Variation to initial measurement (%)	–	–7.0	–7.0	20.9	–7.0
CaCl ₂	ALC10	Measurement	0.59	–	0.80	0.87	1.20
		Variation to initial measurement (%)	–	–	35.6	47.5	103.4
	ALC8	Measurement	0.73	1.02	1.02	1.03	1.00
		Variation to initial measurement (%)	–	39.7	39.7	41.1	37.0
	ALC4	Measurement	0.72	1.14	1.12	1.25	1.25
		Variation to initial measurement (%)	–	58.3	55.6	73.6	73.6
Elastase	ALC7	Measurement	0.86	0.83	0.97	1.03	1.03
		Variation to initial measurement (%)	–	–3.5	12.8	19.8	19.8
	ALC6	Measurement	0.91	1.02	1.10	1.11	1.14
		Variation to initial measurement (%)	–	12.1	20.9	22.0	25.3
	ALC5	Measurement	0.77	0.88	0.88	0.99	0.99
		Variation to initial measurement (%)	–	14.3	14.3	28.6	28.6

**Figure 3.** Biomechanical results: stress (Y axis N/cm²) × strain (X axis) curve displacement towards the origin characterizes lower wall resistance and compliance. (Green: control; red: elastase; blue: CaCl₂).

Biomechanical tests

The aortic wall had lower elasticity, a higher degree of stiffness, and reduced strength in both treatment groups when compared to the non-treated control group (Figure 3). However, displacement and load threshold were both lower in animals treated with CaCl₂. Table 2 shows the reduced threshold in calcium chloride-treated samples. The stress × strain curve shows a shift to the left when compared to control animals.

Histological findings

The CaCl₂ group developed intimal hyperplasia, associated with medial layer muscular and elastic fiber rupture and amorphous matrix deposition (Figure 4G–I). No major inflammatory infiltrate was seen in all wall layers. Elastase-treated samples showed intimal hyperplasia associated with elastic fiber disruption and collagen deposition in the middle wall layer (Figure 4D–F).

Discussion

In this study we describe an endovascular approach that was successful in chemically inducing true aortic aneurysms in medium–large animals. Based on previous models, we compared the effect of two agents to induce aneurysmal dilation.^{2,4} As previously reported, models that use elastase are difficult to reproduce, as the effect of elastase may vary depending on the lot and dose.^{3,5,7,10–12} Elastase also requires proper storage under controlled temperature conditions, is not easily available in many countries, and may need to be associated with other lytic enzymes (collagenase). Conversely, calcium chloride is widely available at local pharmaceutical manufacturers, can be stored at room temperature, is cheap, and has been associated with homogeneous outcomes in the induction of aneurysm. Specifically, it has been shown to induce larger aneurysmal dilations with the formation of wall calcification,^{13–15} as detected by ultrasound and pathological studies. Unfortunately, we observed outcomes associated with severe side effects (livedo, lower limb paraplegia, neurologic bladder, and rectal prolapse) following the use of CaCl₂ 50% with doses greater than 1 mL. These animals were euthanized within 24 hours of the initial surgery. Doppler exams, aortography, and laparotomy revealed patent aorta and iliac vessels. Therefore, these side effects may have resulted from drug washout through lumbar arteries or through the distal balloon. When CaCl₂ was used at a reduced volume and concentration, and the dose split into two, no side effects were seen and calcified and dilated segments were obtained.

Our histological findings indicate that both CaCl₂ and elastase can alter the medial layer of the aortic wall. This layer is responsible for the elastic properties (elastin fibers) as well as the strength (collagen fibers) of the wall.¹⁵ In control animals, the ‘normal’ pattern observed was a monocellular endothelial layer over a thin organized intima. This layer is separated from the medial layer by a single, thin elastic layer, with organized fibers. The

Table 2. Biomechanical test results.

Animal	Group	Failure stress (N/cm ²)	Failure tension (N/cm)	Strain energy (N/cm ²)	Yield tension (N/cm)	F _{max} (N)
ALC1	Control	432.35	43.07	129.5	43.07	13.0
ALC2t	Control	343.74	32.53	94.77	32.53	12.85
ALC2t2	Control	358.87	33.47	102.05	33.47	13.8
ALC4	CaCl ₂	69.78	19.58	22.6	19.58	7.48
ALC8	CaCl ₂	137.18	11.71	33.87	11.71	5.05
ALC10	CaCl ₂	45.12	7.58	6.7	7.58	4.97
ALC5	Elastase	77.12	7.19	31.55	7.19	2.57
ALC6t	Elastase	299.66	26.9	151.54	26.9	10.2
ALC6t2	Elastase	494.16	42.23	142.55	42.23	15.6
ALC7	Elastase	309.62	25.3	164.26	25.3	7.79

T2 represents a second sample of the same animal (2 and 6).

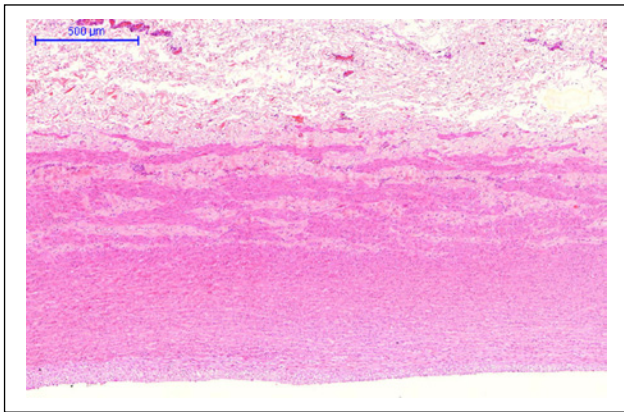


Figure 4A. Control (hematoxylin-eosin) – ‘normal pattern’: monocellular endothelial layer, organized intimal layer; homogeneous and organized elastic fibers; medial muscular layer with organized fibers; adventitia with vasa vasorum and no signs of inflammation.



Figure 4C. Control (Verhoeff) – ‘normal pattern’: organized elastic and muscle layers.

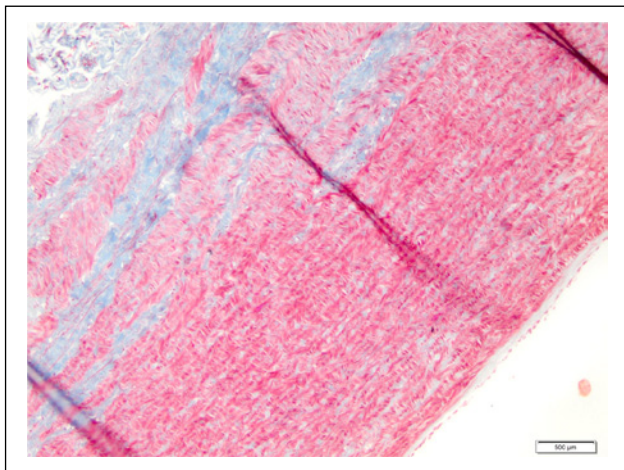


Figure 4B. Control (Masson) – normal wall structure: organized muscle, elastic and collagen fibers.

medial layer contains smooth muscle fibers with little collagen. In the adventitial layer, vasa vasorum is observed (Figure 4A–C).

In elastase-treated samples, endothelial cells are preserved followed by a thickening of the intimal layer due to

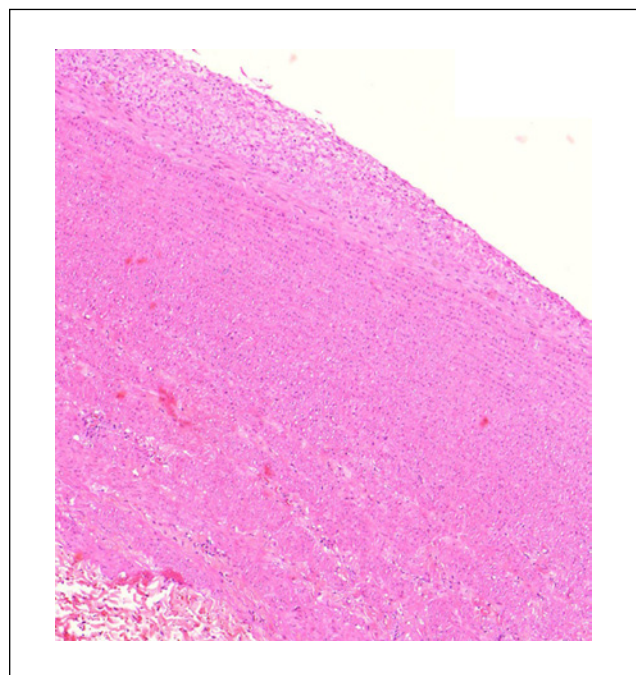


Figure 4D. Elastase (hematoxylin-eosin): fibrointimal hyperplasia.

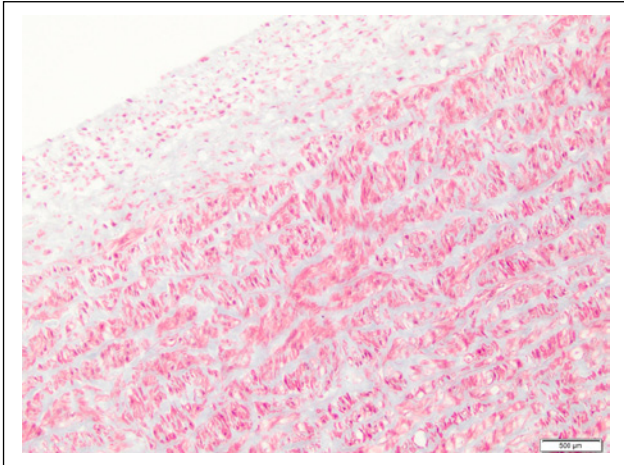


Figure 4E. Elastase (Masson): intimal hyperplasia; unorganized collagen fibers (blue) in the medial layer.

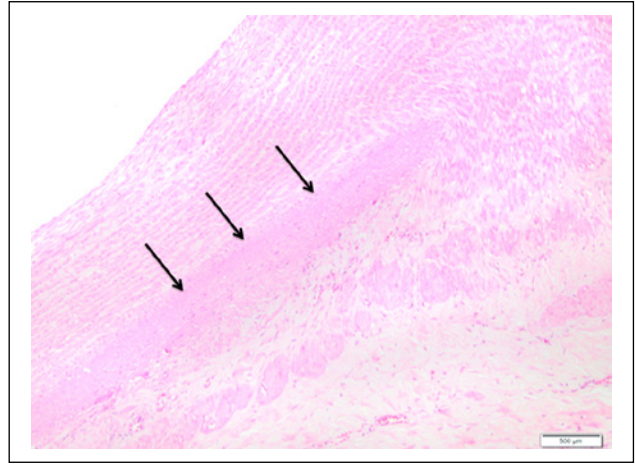


Figure 4G. Calcium chloride (hematoxylin-eosin): intimal hyperplasia; unorganized middle layer with replacement of muscle cells by amorphous matrix and area of calcification (arrows) (40×).

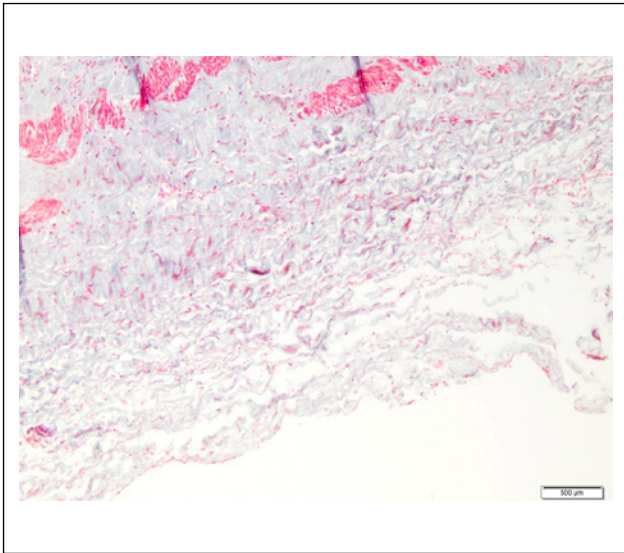


Figure 4E1. Normal aspect of the adventitia – no inflammatory cells are seen (Masson, 100×).

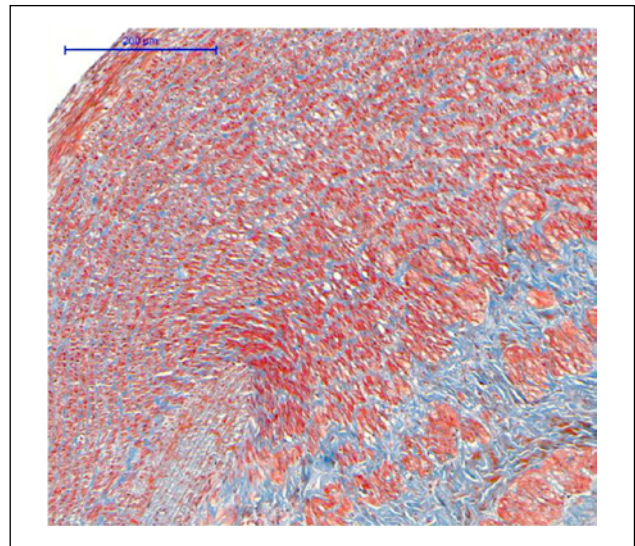


Figure 4H. Calcium chloride (Masson): unorganized limitant elastic layer, unorganized muscle cells, amorphous matrix deposition.

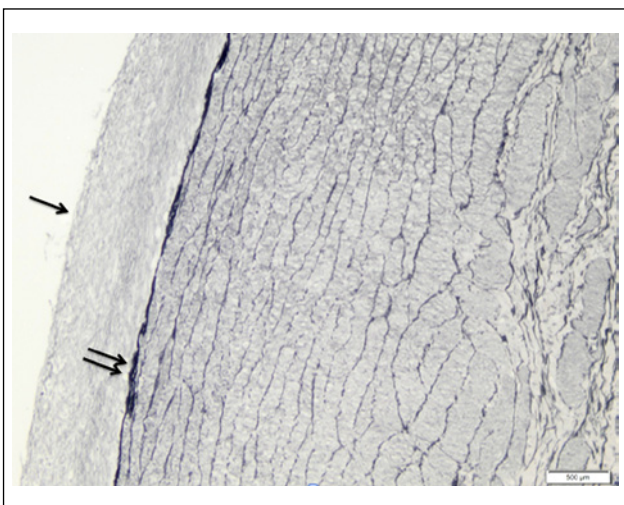


Figure 4F. Elastase (Verhoeff): irregular and delaminated elastic fibers (double arrows); intimal hyperplasia (single arrow).

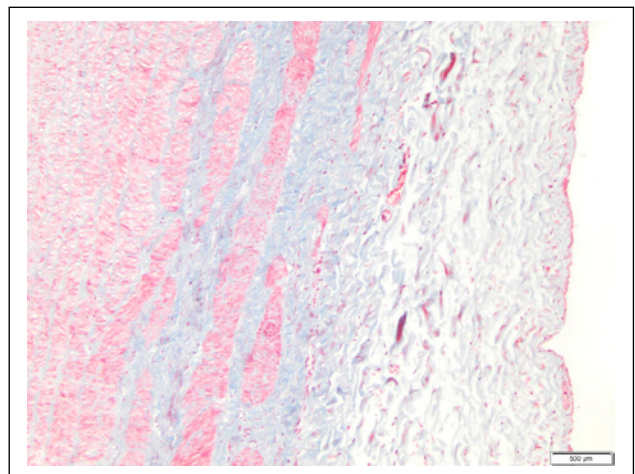


Figure 4H1. Amorphous matrix deposition – no inflammatory cells in the adventitia.

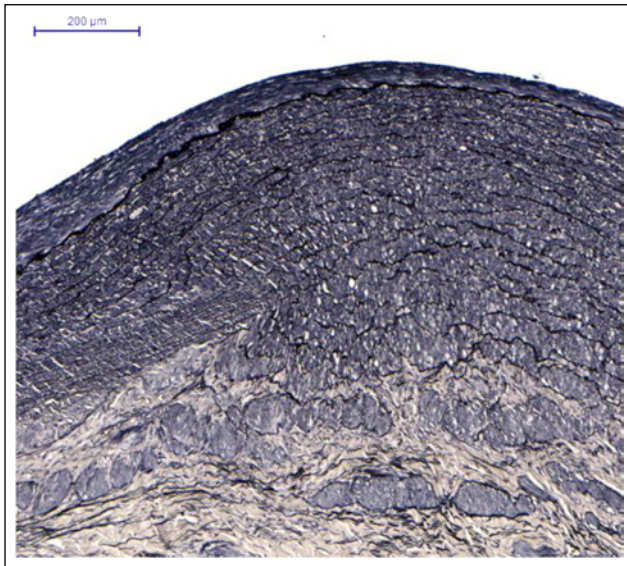


Figure 4I. Calcium chloride (Verhoeff): unorganized limitant elastic layer, unorganized muscle cells, amorphous matrix deposition.

collagen fiber growth. The elastic lamina is irregular, fragmented, and delaminated. Muscle fibers have been replaced by unorganized collagen fibers in the middle layer. The adventitia is maintained and shows no inflammatory response (Figure 4D–F).

Calcium chloride-treated samples had to be treated to have the calcium removed with formic acid 20% (O Artifice, São Paulo, Brazil) exposure for 1 hour, prior to beginning histological preparation for block inclusion and cutting. Histological analysis shows a monocellular endothelial layer, with a fibro-intimal thickening that is coincident with elastic delamination and rupture. Muscle fibers are scarce, there is deposition of amorphous material, and medial calcification is seen (vacuoles as a result of the decalcification treatment). The adventitial layer is preserved (Figure 4G–I).

Even though most previously described models require an inflammatory response, we did not observe such a response in the adventitial aortic layer.^{7,16} This fact may be associated with the nature of the endovascular approach.

To determine aortic wall changes and dilation, weekly ultrasound examinations were done. Ultrasound proved to be a good method for follow-up. Even though animals must be sedated or anesthetized, aortic changes, dilation, calcification, and blood flow developments were seen in real time. Here we show that CaCl_2 had already induced initial dilation and wall calcification within the first week. After 2 weeks, it was possible to consider the dilation to be an aneurysm (>50%). Unfortunately, we cannot establish whether there would be further increase and rupture after 4 weeks, when our animals were euthanized.

Our biomechanical test results (Table 2) have proven that the aortic wall changes observed caused wall weakness and lower elasticity, making the samples more prone to rupture, particularly when CaCl_2 was used. This response pattern – stress \times strain curve shift to the left – is similar to the one found^{17,18} when these authors compared normal to

aneurysmal aortas in humans. This similarity indicates that our model is representative of a true aneurysm.

Previous experimental data show that aneurysm induction is feasible through direct aortic access and manipulation. This process involves physical and chemical trauma of the aortic wall, leading to arterial wall thinning and dilation. As a natural healing process, retroperitoneal fibrosis develops as a fibrous hardened scar tissue is formed surrounding the dissected aorta. This healing process is not desired when using models to train new surgeons, since it presents technical difficulties not usually encountered in real-life situations. Also, lumbar arteries are ligated during dissection. This procedure diminishes physiological similarities, which may be a problem when studying endoleaks in new stenting devices. In this study, we showed that the use of an endovascular approach enabled us to induce an aortic wall lesion without the need for surgical dissection. As expected, lumbar arteries remained patent and no fibrosis around the aortic wall was seen during harvesting of our samples.

We used two Fogarty catheters and a microcatheter technique to induce the aneurysms. Today, an off-the-shelf single catheter with two occluding balloons and working lumen (TAPAS[®]; ThermopeutiX Inc., San Diego, CA, USA) is available that enables reproduction of our procedure using a single element. This might make our technique easier to repeat.

Our sample size is small and a larger sample may be more convincing of the results obtained. On the other hand, one should be concerned with excessive use of animals. Laboratory animals are expensive to acquire and maintain, and the procedure is invasive and requires postoperative monitoring. Also, all calcium chloride-treated animals developed the same pattern of arterial wall change: calcification and dilatation. Therefore, even though we would have liked to operate on more animals, we could not support doing so since we had achieved our goal of creating an endovascular model for aneurysm development. In regard to a large population series, we believe that results should also be similar. For comparison, Czerski et al.⁷ used a sample of four animals in each group for their study on aneurysm creation.

Conclusion

To our knowledge, this is the first endovascular model of true AAA and the first model to date tested for biomechanical properties, which have been shown to be similar to those of human AAA. Calcium chloride seems to be an easy and cheap way to obtain AAA. The endovascular approach is feasible and produces no retroperitoneal fibrosis around the aneurysms.

Acknowledgements

We thank Timothy Chung, University of Iowa, who developed and verified the matlab algorithm used for calculating mechanical properties from mechanical test data; Elivane da Victor, Centro de Pesquisa Clínica, Estatística Instituto Israelita de Ensino e Pesquisa – IIEP, who helped with data analysis; and Valéria Vieira

Chida, Instituto Israelita de Ensino e Pesquisa Albert Einstein – Centro de Experimentação e Treinamento em Cirurgia, who was responsible for animal care and anesthesia. This manuscript was reviewed by a professional science editor and by a native English-speaking copy editor to improve readability.

Declaration of conflicting interest

The authors have no conflict of interest to declare.

Funding

This work was supported by FAPESP (Fundação de Amparo a Pesquisa do Estado de São Paulo) (grant number 2010/07307-6).

References

- Molacek J, Treska V, Kobr J, et al. Optimization of the model of abdominal aortic aneurysm – experiment in an animal model. *J Vasc Res* 2009; 46: 1–5.
- Conn PM. *Sourcebook of Models for Biomedical Research*. Totowa, NJ: Humana Press, 2008.
- Anidjar S, Salzman JL, Gentric D, Lagneau P, Camilleri JP, Michel JB. Elastase-induced experimental aneurysms in rats. *Circulation* 1990; 82: 973–981.
- Argenta R, Pereira AH. Modelos animais de aneurisma de aorta. *J Vasc Bras* 2009; 8: 148–153.
- Hynecek RL, DeRubertis BG, Trocciola SM, et al. The creation of an infrarenal aneurysm within the native abdominal aorta of swine. *Surgery* 2007; 142: 143–149.
- Trollope A, Moxon JV, Moran CS, Golledge J. Animal models of abdominal aortic aneurysm and their role in furthering management of human disease. *Cardiovasc Pathol* 2011; 20: 114–123.
- Czerski A, Bujok J, Gnus J, et al. Experimental methods of abdominal aortic aneurysm creation in swine as a large animal model. *J Physiol Pharmacol* 2013; 64: 185–192.
- Sincos IR, Aun R, da Silva ES, et al. Impact of stent-graft oversizing on the thoracic aorta: experimental study in a porcine model. *J Endovasc Ther* 2011; 18: 576–584.
- Raghavan ML, Hanaoka MM, Kratzberg JA, de Lourdes Higuchi M, da Silva ES. Biomechanical failure properties and microstructural content of ruptured and unruptured abdominal aortic aneurysms. *J Biomech* 2011; 44: 2501–2507.
- Kratzberg JA, Walker PJ, Rikkers E, Raghavan ML. The effect of proteolytic treatment on plastic deformation of porcine aortic tissue. *J Mech Behav Biomed Mater* 2009; 2: 65–72.
- Sadek M, Hyneczek RL, Goldenberg S, Kent KC, Marin ML, Faries PL. Gene expression analysis of a porcine native abdominal aortic aneurysm model. *Surgery* 2008; 144: 252–258.
- Carsten CG, Calton WC, Johanning JM, et al. Elastase is not sufficient to induce experimental abdominal aortic aneurysms. *J Vasc Surg* 2001; 33: 1255–1262.
- Gertz SD, Kurgan A, Eisenberg D. Aneurysm of the rabbit common carotid artery induced by periarterial application of calcium chloride in vivo. *J Clin Invest* 1988; 81: 649–656.
- Chiou AC, Chiu B, Pearce WH. Murine aortic aneurysm produced by periarterial application of calcium chloride. *J Surg Res* 2001; 99: 371–376.
- Maier A, Gee MW, Reeps C, Eckstein HH, Wall WA. Impact of calcifications on patient-specific wall stress analysis of abdominal aortic aneurysms. *Biomech Model Mechanobiol* 2010; 9: 511–521.
- Anidjar S, Dobrin PB, Eichorst M, Graham GP, Chejfec G. Correlation of inflammatory infiltrate with the enlargement of experimental aortic aneurysms. *J Vasc Surg* 1992; 16: 139–147.
- Tavares Monteiro JA, Simão da Silva E, Raghavan ML, Puech-Leão P, Higuchi MD, Otoch JP. Histological, histochemical and biomechanical properties of fragments isolated from the anterior wall of abdominal aortic aneurysms. *J Vasc Surg*. Epub ahead of print 24 Jul 2013. DOI: 10.1016/j.jvs.2013.04.064.
- Raghavan ML, Webster MW, Vorp DA. Ex vivo biomechanical behaviour of abdominal aortic aneurysm: Assessment using a new mathematical model. *Ann Biomed Eng* 1996; 24: 573–582.